Solar Cells, 31 (1991) 223–236

Determination of lifetime and surface recombination velocity in solar cells

J. M. Salagnon and **S. Mouhammad**
Laboratoire de Physique de l'Etat Solide, I.S.S.A.T. B.P. 70 28 Damascus (Syria)

P. Mialhe
Laboratoire de Physique du Solide, Université de Perpignan, Avenue de Villeneuve, 66025 Perpignan (France)

F. Pelanchon
CEDUST, Ambassade de France, B.P. 39 29 Damascus (Syria)

(Received July 17, 1990; in revised form December 8, 1990)

Abstract

A detailed theoretical analysis was made of a new experimental practice for determining the minority carrier lifetime τ_n and the back surface recombination velocity S_B in silicon solar cells by the short circuit current decay method. The measurements were taken by monitoring both the current–voltage characteristic and a single transient of an operating cell at any level of injection when no power supply is required. The complete continuity differential equation for minority carrier transport including the generation rate of carriers is considered. A practicable analytical expression of the current response is derived and the analysis includes both thick and thin base cells. Good precision and sensitivity are obtained for actual high quality solar cells and a lower precision appears for high values of both τ_n and S_B (τ_n greater than the extrinsic lifetime value as defined by the Shockley–Read–Hall recombination process, S_B greater than 10^4 cm/s). Experimental results are presented to support the mathematical analysis.

1. Introduction

Experimental methods have been used to determine the carrier lifetime in the base region of solar cells. For these methods [1] a steady state is abruptly terminated and the transient response of the open circuit voltage (V_{oc}) or of the short circuit current (I_{sc}) is measured; they are based on the interpretation of the shape of the decay curves, as the reciprocal of the slopes for a straight line shape, or the time constant for an exponential shape, are related to the minority carrier lifetime. It is well known that the values of carrier lifetime determined by different experimental methods are not the same.

Theoretical results differ with the excitation used to obtain the steady state and show that the shape of the decay curve is dependent on unknown parameters such as the diffusion coefficient [2–4], diffusion length [5], surface recombination velocity [3, 4, 6] or diode ideality factor [7]. Experimental

0379-6779/91/$3.50

conditions affect the decay curve [8]. There are also parasitic impedance [9–12] and injection level effects [7, 13–17]. Of the many variations of the transient techniques for measuring minority carrier lifetime and surface recombination velocity, the short circuit current decay method is of particular interest since it avoids junction capacitance effects. Until now, no theoretical expression of the transient short circuit current as a function of time has been derived for a solar cell operating under illumination.

The aim of this work is to suggest a new experimental use of the short circuit current decay method [2, 18] for the determination of back recombination velocity and base minority carrier lifetime of crystalline solar cells. It requires the observation of only a single transient of an operating solar cell under real conditions at any level of carrier injection, together with the whole *I–V* characteristic. This technique is more accurate than that previously reported since it does not need an applied bias or a variation of the generation rate of carriers due to illumination (referred to as the Constant Illumination Short Circuit Current Decay (CISCCD) method). For this purpose, we have developed a mathematical model which takes into account the carrier generation rate and the dielectric relaxation. The application of this analysis is illustrated by experimental measurements with high quality commercial solar cells.

2. Theory

A solar cell is illuminated with a steady photon flux, the operating point is represented in Fig. 1 (point O), which defines the initial steady state. At time $t=0$, a MOS-transistor switch (characteristic switching time 30 ns; on-state resistance $<0.2\ \Omega$) (Fig. 2) removes the load resistor R and the small external resistor R_o, used to monitor the transient current, nearly provides a short circuit. To analyse the transient current we have to solve the time dependent diffusion equation for the excess minority carrier concentration $n(x,t)$ in the base (p-type) region:

$$D_n \partial^2 n(x,t)/\partial x^2 + G(x) - \partial n(x,t)/\partial t = n(x,t)/\tau_n \tag{1}$$

where $G(x)$ is the carrier generation rate, D_n is the electron diffusion coefficient and τ_n is the electron lifetime.

A solution of eqn. (1) for the transient state, which we have considered, may be obtained in the following manner. The carrier concentration at time t may be written:

$$n(x,t) = n_s(x) + \delta(x,t) \tag{2}$$

where $n_s(x)$ is the steady state concentration value under short circuit conditions (operating point S in Fig. 1, that is the final steady state at $t=\infty$). The junction plane is situated at $x=0$ and the back surface at $x=H$. Concentration $n_s(x)$ satisfies the steady state diffusion equation:

$$D_n \partial^2 n_s(x)/\partial x^2 + G(x) = n_s(x)/\tau_n \tag{3}$$

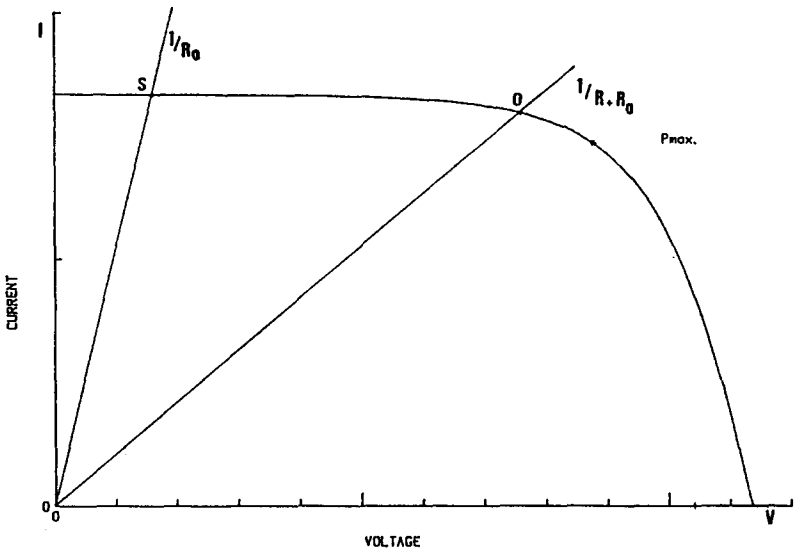

Fig. 1. Solar cell *I–V* characteristic and operating points S and O with load resistors R_O and $R+R_O$.

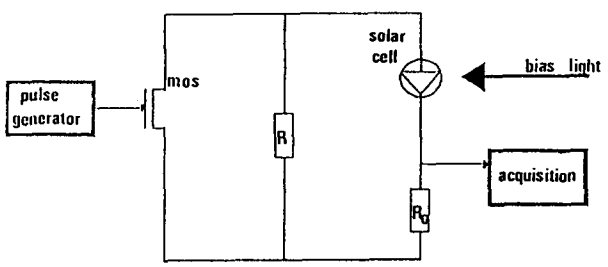

Fig. 2. Experimental set-up.

The observed transient current results from the decrease of the injected carrier concentration which follows the fast switching at time $t=0$. Since the solar cell operates at every time under the same illumination level, no change in recombination rates is expected in the bulk of the base after a time longer than several dielectric relaxation times. Inserting eqn. (2) in eqn. (1) we find that the excess carrier concentration $\delta(x,t)$ is a solution of the differential equation

$$D_n\partial^2\delta(x,t)/\partial x^2 - \delta(x,t)/\tau_n = \partial\delta(x,t)/\partial t \qquad (4)$$

At time $t=0$ the fast switching makes coincident the quasi-Fermi levels at the front and back metal contacts [2] and the junction voltage gets its equilibrium value ($t=\infty$), within a time lower than $10^{-4}\ \tau_n$ which may be called a re-adjustment time noted 0^+. As a consequence of this re-adjustment effect, produced by dielectric relaxation, the excess carrier concentration δ

drops abruptly to zero at the edge of the space charge region. The transient state, that we observe, follows junction barrier and carrier density readjustments. Then it is obvious that $\delta(x,0^+)=\delta(x,0)$ for $x>0$.

The boundary conditions for the solution of eqn. (4) are as follows:

$$\delta(0,\,t)=0 \quad (t>0) \tag{5}$$

$$\partial\delta(H,\,t)/\partial x=-S_B\delta(H,\,t)/D_n \tag{6}$$

$$\delta(0,\,0)=\delta_\phi \tag{7}$$

where eqn. (5) represents the short circuit condition, S_B is the back surface recombination velocity and δ_ϕ depends on both the initial and the final steady states. Note that eqns. (5) and (7) point out that function $\delta(x,t)$ is discontinuous for $(x=0,\ t=0)$.

The complete solution of eqn. (4) subject to these boundary conditions may be obtained through the same mathematical analysis for infinite or finite base width (see Appendix). For $t>0$ we get:

$$\delta(x,t)=\delta_\phi\sum_{p\geq 1}\frac{\Omega_p}{a_p}\,\frac{\sqrt{D_n}}{1/\tau_n+\Omega_p{}^2}\,\sin((\Omega_p/\sqrt{D_n})x)\,\exp(-(1/\tau_n+\Omega_p{}^2)t) \tag{8}$$

The simplicity of this expression results from the boundary conditions (5)–(7) our experimental method imposed. This experimental method makes it possible to derive such a result by using the same illumination level in both the initial and the final states.

Using

$$I_{sc}(t)=q\,D_n\partial n(x,t)/\partial x|_{x=0} \tag{9}$$

we find the time dependence $i(t)$ $(t>0)$ of the short circuit current I_{sc} as:

$$i(t)=\sum_{p\geq 1} i_p(t) \tag{10}$$

with

$$i_p(t)=q\,\delta_\phi\,\frac{1}{a_p}\,\frac{\Omega^2{}_p}{1/\tau_n+\Omega^2{}_p}\,D_n\,\exp(-(1/\tau_n+\Omega^2{}_p)t) \tag{11}$$

The series expansion in eqn. (10) converges uniformly for $t>0^+$. Figure 3 shows plots of the transient current $i(t)$ against normalized time t/τ_n: curves 1 to 10 were obtained when considering a limited part of the series expansion (eqn. (10)), respectively one term, two terms, ..., ten terms. Figure 3 illustrates the convergence of the series expansion: the first term dominates higher ones for reduced time values greater than 1/2. Values of δ_ϕ and S_B were found to be not sensitive and the series converges more rapidly for a thin base cell (Fig. 3(a)) than for a thick base cell (Fig. 3(b)), a result also observed in previous works with different experimental techniques. The following result holds for the most unfavorable case of a thick base cell ($H=300$ μm, base doping $N_B=8\times10^{16}$ cm^{-3} (minority carrier diffusion length of 100 μm)):

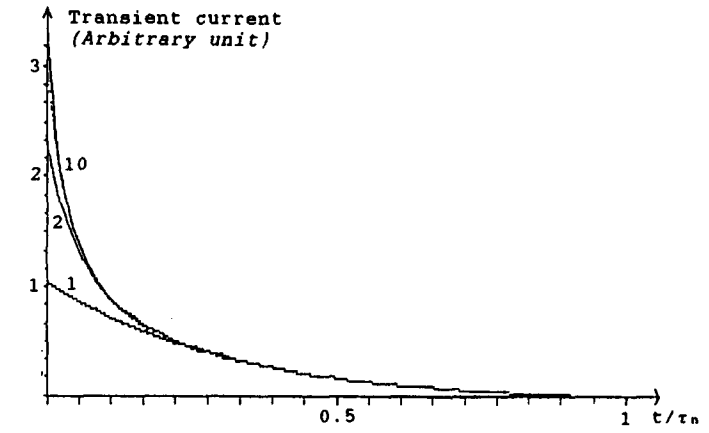

(a)

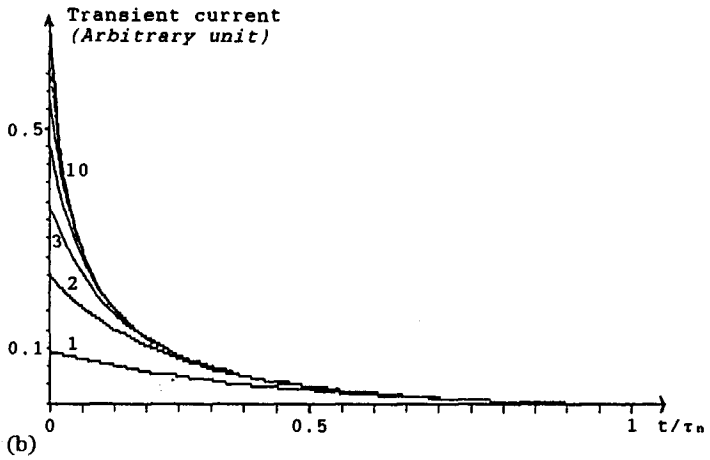

(b)

Fig. 3. Transient current plotted as a function of normalized time t/τ_n. The convergence of the series expansion (sum for $i=1$ to p) is shown: curve 1 ($p=1$, first term), curve 2 ($p=2$), ... , curve 10 ($p=10$). (a) $N_B=10^{16}$ cm^{-3}, $H=200$ μm, $S_B=10^2$ cm s^{-1}; (b) $N_B=8\times10^{16}$ cm^{-3}, $H=300$ μm, $S_B=5\times10^5$ cm s^{-1}.

$$i(\tau_n)=1.074\ i_1(\tau_n)$$

Higher terms contribute only by 7.4% to the decay current at $t=\tau_n$.

The shapes of the profiles of the excess carrier concentration $\delta(x,t>0)$ were calculated using eqn. (8) and are plotted in Fig. 4 at several time values during the initial stage of the decay. The profiles show a maximum value, the magnitude of which points out that high injection effects cannot be studied in this way. The maximum moves away from the junction and broadens as time increases (as reported for the whole excess minority carrier charges [9]). At a time t within lifetime τ_n, the excess concentration near the junction becomes insignificant for both conventional cells (Fig. 4(a)) and

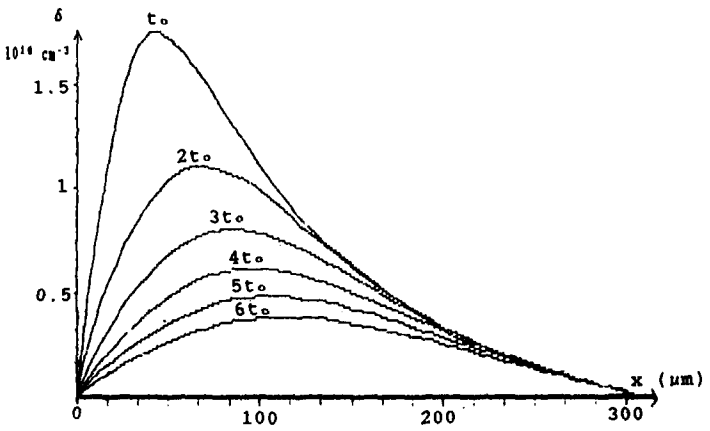

(a)

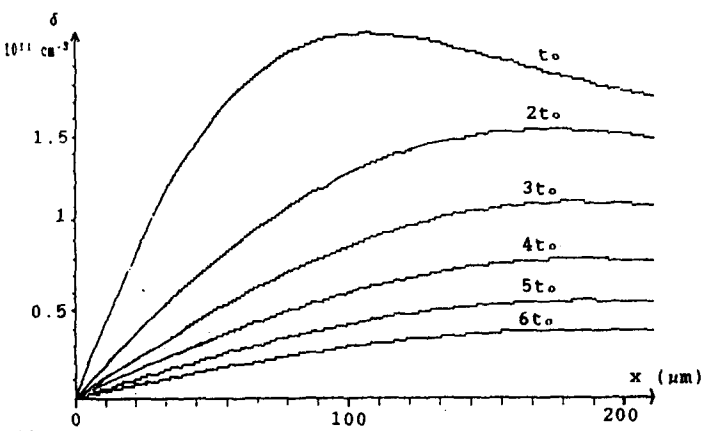

(b)

Fig. 4. (a) Profile of excess carrier concentration $\delta(x,t)$ plotted as a function of x for different values of time (as shown on the curves, $t_o = \tau_n/20$): (a) $N_B = 10^{17}$ cm^{-3}, $H = 300$ μm, $S_B = 10^7$ cm s^{-1}; (b) $N_B = 10^{16}$ cm^{-3}, $H = 200$ μm, $S_B = 5 \times 10^2$ cm s^{-1}.

back surface field cells (Fig. 4(b)), implying negligible effect of the emitter on the observed decay curve. The forward emitter current and the reverse base current necessary in the initial stage are negligible at $t \geq \tau_n$ since the lifetime of the minority carriers, on the emitter side, is shorter than the minority carrier lifetime on the base side.

These results show that the series expansion of eqn. (10) can be reduced to one term after the initial stage of the decay curve:

$$i(t) = \delta_\phi F(t_n, \Omega) \exp(-t/\tau_{SC}) \tag{12}$$

where

$$F(\tau_n, \Omega) = q \frac{(\Omega^2 D_n)/(\Omega^2 + 1/\tau_n)}{H/2 - \frac{1}{4}\sqrt{D_n}/\Omega \sin(2(\Omega/\sqrt{D_n})H)} \tag{13}$$

$$1/\tau_{SC} = \Omega^2 + 1/\tau_n \tag{14}$$

$$\tan(\Omega H/\sqrt{D_n}) = -\sqrt{D_n}\,\Omega/S_B, \qquad \pi/2 < \Omega H/\sqrt{D_n} \leq \pi \tag{15}$$

Equation (12) contains four unknown parameters: δ_ϕ, Ω, τ_n and S_B. The time constant (τ_{SC}) of the transient current is measured. $i(0)$ and δ_ϕ, related to the initial and final states, are determined by experiments (to be discussed below) that leads to the value of Ω. Then eqns. (14) and (15) yield, respectively, the values of the desired parameters τ_n and S_B.

3. Experimental method and procedures

3.1. Transient short circuit current curve

The transient terminal voltage was monitored using a computerized data acquisition system. Figure 5 displays the short circuit current decay curve together with a semi-logarithmic plot which illustrates the exponential decay obtained at $t > \tau_{SC}$. For large values of t, the signal to noise ratio is low and measurements are not accurate. A numerical procedure allows the determination of both τ_{SC} and $i(0)$. (Note that dielectric relaxation process produces a large perturbation of the initial stage of the decay curve that introduces

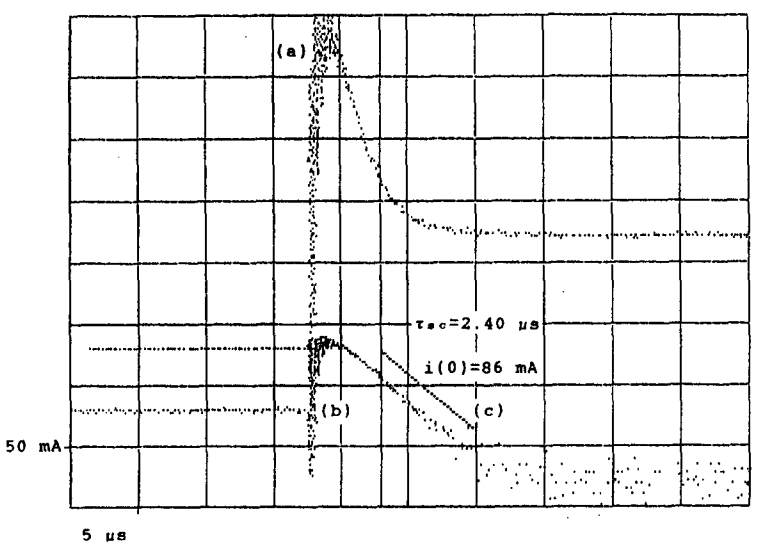

Fig. 5. Experimental transient decay: (a) short circuit current; (b) semi-log scale representation of (a); (c) linear regression of (b).

a systematic error in the experimental value of time t and yields inaccurate measurements of $i(0)$ from the extrapolated intercept at time $t=0$).

3.2. Elimination of junction voltage measurements

The parameter δ_ϕ, related to both the initial and the final steady states, strongly depends on the junction voltage (V_d) and no accurate experimental determination of this voltage is available. This fact has been discussed by some authors [2, 4, 12, 18]. They eliminated the need for this voltage measurement by performing experiments with different illumination or injection levels, but introduced new uncertainties that made their method impractical in manufacturing. An accurate value of δ_ϕ may be obtained from a study of the *I-V* characteristic of the device, as shown below.

From modelling studies [20] we know that currents I_O and I_S at operating points O and S satisfy:

$$I_O = I_{ph} - I_r(\exp(V_{dO}/(V_T A)) - 1) \tag{16}$$

$$I_S = I_{ph} - I_r(\exp(V_{dS}/(V_T A)) - 1) \tag{17}$$

where V_{dO} (V_{dS}) is the junction potential at operating point O (S). I_{ph} is the photocurrent, I_r the reverse diode current, V_T the usual thermal potential and A the cell quality factor. Using general semiconductor physics [21]:

$$\delta_\phi = n_i^2/N_B\ (\exp(V_{dO}/V_T) - \exp(V_{dS}/V_T)) \tag{18}$$

where n_i is the intrinsic carrier concentration.

Taking into account that the cell is short-circuited in the final state, the substitution of eqns. (16) and (17) in eqn. (18) eliminates the unknown junction voltages. We get:

$$\delta_\phi = n_i^2/N_B((I_S - I_O)/I_r)^A \tag{19}$$

It is possible to determine δ_ϕ as soon as the values of I_S, I_O and I_r are obtained: I_O and I_S are measured and the fit of the whole I–V characteristic by using the first order one diode model [20] enables us to determine I_r. Note that a direct calculation of $I_O - I_S$ as a function of δ_ϕ, from eqn. (9), is not possible because the series expansion (eqn. (8)) does not converge at $t=0$ (that comes from the discontinuity of function δ, introduced to take into account dielectric relaxation).

This procedure eliminates the necessity of a junction potential measurement and the method considers the emitter recombination current since the pre-exponential factor I_r contains two components, $I_r = I_{rb} + I_{re}$, where I_{rb} is the base saturation current and I_{re} is the emitter component.

3.3. Measurement of parameter Ω

Figure 6 displays the graph of function $F(\tau, \Omega)$ when Ω is varying in the restricted interval $\sqrt{D_n}/H(\pi/2, \pi)$ (see eqn. (A6)), obtained by using some values of the unknown parameter τ. The intersections of the straight line $i(O)/\delta_\phi = \text{constant}$ with $F(\tau, \Omega)$ curves introduce several roots $(\tau, \Omega)_i$ and the single physical solution (τ_n, Ω') (verifying eqn. (14)) may be selected

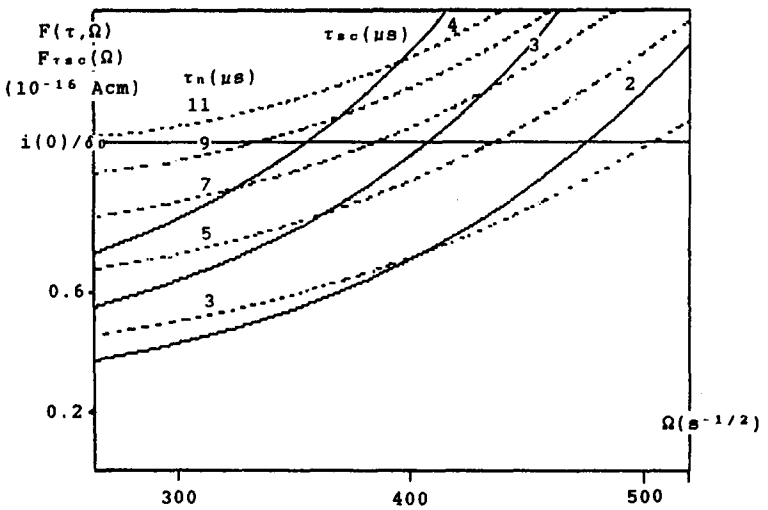

Fig. 6. Graphs of functions $F(t,\Omega)$ (dashed lines) and $F_{\tau_{sc}}(\Omega)$ (solid lines) against Ω, for several values of parameter τ and decay times τ_{sc}, respectively; the intercept with the straight line $i(O)/\delta_\phi$ is shown. ($N_B = 5\times10^{16}$ cm^{-3}, $H = 300$ μm.)

from the intercept of this straight line with the curve $F\tau_{SC}(\Omega)$, where $F\tau_{SC}(\Omega) = F((\tau_{SC}{}^{-1} - \Omega^2)^{-1}, \Omega)$.

In practice, the $F\tau_{SC}(\Omega)$ curve may be drawn alone and the intercept with the straight line leads to the value Ω', which is used to compute the carrier lifetime τ_n from eqn. (14). Assuming that the precision of the determination of the ratio $i(O)/\delta_\phi$ is 10%, the error in the value Ω' of parameter Ω coming from this graphical measurement is $\Delta\Omega' = 40\ s^{-1/2}$.

3.4. Measurements of lifetime and surface recombination

Figure 7 is a plot of τ_n against Ω, obtained from eqn. (14) (Ω being varied in its restricted interval), for several values of the measured short circuit decay time τ_{SC}. The precision of the determination of lifetime τ_n is better for low values of parameter Ω than for values close to its upper bound when τ_n is larger than τ_{SC}. In this last case, the uncertainty in the value of Ω contributes more to the error than does the uncertainty in the decay time constant value.

The back surface recombination velocity is obtained from the roots of the eigenvalue of eqn. (15) which is illustrated in Fig. 8. The thin base solar cells, i.e. with base width of the order of base diffusion length, are considered (Fig. 8(a)) and Fig. 8(b) shows that, as the base width increases, both Ω and the magnitude of its restricted interval decrease to a small value comparable to $\Delta\Omega$, making the determination of S_B impossible. From physical consideration, this result can be understood: when the base width is much greater than the base diffusion length (thick base solar cell), the back surface recombination becomes insignificant, since most of the minority carriers recombine before

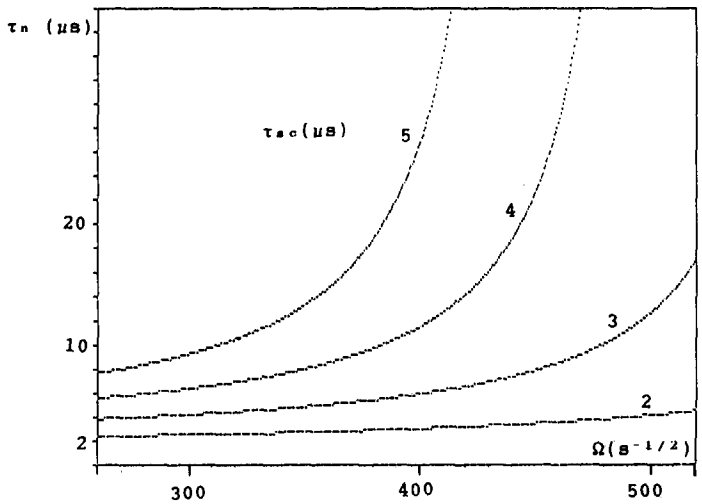

Fig. 7. Plot of minority carrier lifetime as a function of Ω, for several values of decay times τ_{sc}. ($N_B = 5 \times 10^{16}$ cm^{-3}, $H = 300$ μm.)

they reach the back surface. Figures 8(a) and 8(b) show, in the opposite case, that large values of Ω are obtained for low doping levels (large D_n values) and when the base width decreases. In this case, both the lifetime and the back recombination velocity are well determined.

4. Experimental results and discussion

We illustrate the method with results for two cells for which the parameters are given in Table 1 (a fitting process [20] of the whole I–V characteristic has been used to compute series resistances, quality factors and reverse diode currents). They are silicon commercial blue solar cells for terrestrial use: the emitter region is made fairly thin (0.1–0.2 μm) of n^+-type, the emitter surface is oxide passivated to reduce surface recombination and grid contact recombination is lowered by reducing the metal–silicon area; the base is of p-type.

Table 2 shows the experimental parameters along with the values of minority carrier lifetimes in the base and of back surface recombination velocities derived for the two cells. The precision is obtained with a computer process which takes into account the criterion of effectiveness [20] in the description of the I–V characteristic, the precision in the computer measured decay parameters and the following uncertainty in the determination of the cell parameters: cell width (5%) and base doping (30%).

Cell 1 exhibits a value of base carrier lifetime shorter than the extrinsic value of 12 μs for this base doping level value which corresponds to a diffusion length of 90 μm. It is a confirmation of the low quality of this cell (11% measured efficiency). In this case a larger back recombination velocity

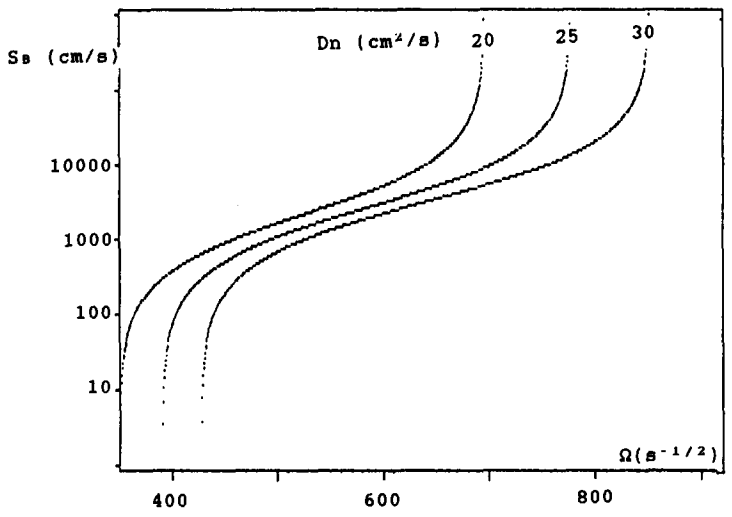

(a)

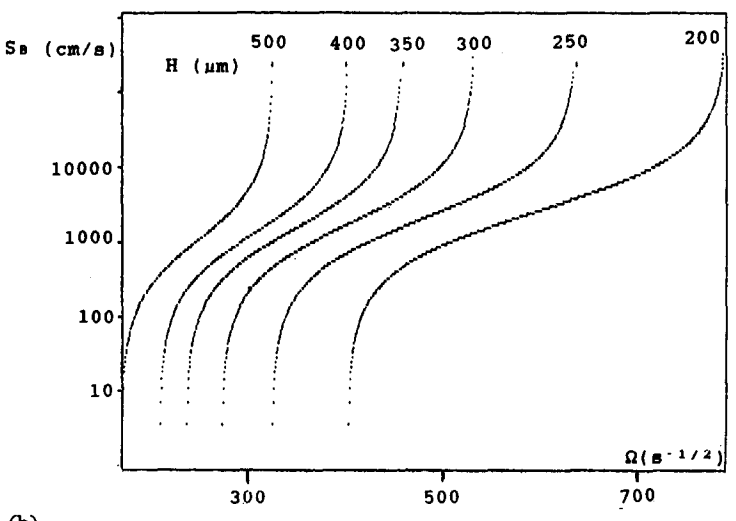

(b)

Fig. 8. Plot of back surface recombination velocity as a function of Ω, for several values of (a) diffusion coefficient D_n ($H=200$ μm); (b) base width H ($N_B=5\times10^{16}$ cm^{-3}).

should be expected since few carriers can reach the back surface. The high quality of cell 2 may be stated, and the large value of its reverse diode current (I_r) shows, that a further improvement of its efficiency is related to a decrease of I_r. Moreover, this decrease should be correlated to the structures of both emitter and space charge region.

These results enable an evaluation of the uncertainty in the direct [4] junction voltage determination for which the series resistance R_s of the device

TABLE 1. The cell parameters

Cell	H (μm)	N_B (cm^{-3})	Area (cm^2)	R_s (Ω)	A	I_r (A)
1	320	10^{15}	6	0.26	1.52	6.9×10^{-8}
2	320	10^{16}	3.5	0.54	1.74	1.9×10^{-7}

TABLE 2. CISCCD measurements for two solar cells

Cell	τ_{sc} (μs)	i(O) (mA cm^{-2})	δ_ϕ (cm^{-3})	τ_n (μs)	S_B (cm 0000s^{-1})
1	1.5	18	1.0×10^{14}	2.9	8.3×10^4
				(0.3)	(2100)
2	7.1	6.3	3.3×10^{13}	22.5	375
				(2.5)	(30)

The numbers in parentheses are the precision of the data.

must be taken into account to correct for voltage drops. With experiments on device 1 the short circuit current was $I_{SC}=127$ mA, that is a 33 mV drop to be compared with the operating voltage $V_O=470$ mV. An inaccurate value of R_s, say $\Delta R_s=0.1$ Ω, yields an uncertainty in the direct determination of parameter δ_ϕ with eqn. (18), $\Delta\delta_\phi/\delta_\phi=0.5$.

Compared with previous experimental procedures [2–4, 18] on short circuit current transients (which can be applied only to thin base solar cell), the CISCCD method is more general since it applies whatever be the ratio (greater than 1/4) of carrier diffusion length to base width for high performance solar cells. The differences are caused by our experimental procedure that leaves the cell under a constant illumination level. In previous procedures, applied forward bias or light pulses were required, that produced a strong discontinuity in carrier transport mechanisms, compared with the weak disturbance imposed to the cell when the CISCCD method is used. The proposed method avoids parasitic impedance effects since the illumination level is not varied before and during the transient event. No power supply is required [22].

5. Conclusion

We have given a detailed analysis of the CISCCD method of lifetime and surface velocity measurements. The first expression of a transient short circuit current of a solar cell under illumination has been derived for any illumination level. We have shown that the transient current decays directly corresponding to $\exp(-t/\tau_{sc})$ after the initial stage of the transient event. This result holds for both thin and moderately thick devices (that is for a 300 μm base thickness, a doping level lower than the optimum 10^{17} cm^{-3}

value [23]). The difference between the ESCCD [2] and CISCCD method comes from the constant illumination level used in the latter which allows for a slight experimental perturbation of the operating conditions to get the transient state. Furthermore, for solar cells, the carrier profiles obtained by this method are more realistic than those obtained from carrier injection by an electric pulse. The method enables us to determine the minority carrier lifetime in the base and the back surface recombination velocity.

The authors are grateful to Dr. J. P. Charles who made possible parameter determinations with his computer process.

References

1 S. R. Dhariwal and N. K. Vasu, *Solid-State Electron, 24* (1981) 915–927.
2 T. W. Jung, A. Lindholm and A. Neugroshel, *IEEE Trans. Electron Devices, 31* (1984) 588–595.
3 B. H. Rose and H. T. Weaver, *Proc. 17th IEEE Photovoltaic Specialists' Conf., 1984 IEEE, Kissimmee, 1–4 May, 1984*, pp. 626–631.
4 A. Zondervan, L. Verhoef, F. A. Lindholm and A. Neugroshel, *J. Appl. Phys., 63* (1988) 5563–5570.
5 S. C. Jain, *Solid-State Electron., 24* (1981) 179–183.
6 B. H. Rose and H. T. Weaver, *J. Appl. Phys., 54* (1983) 238–247.
7 K. Joardar, R. C. Dondero and D. K. Schroder, *Solid-State Electron., 32* (1989) 479–483.
8 P. Mialhe, G. Sissoko and M. Kane, *J. Appl. Phys., 20* (1987) 762–765.
9 M. A. Green, *Sol. Cells, 11* (1984) 147–161.
10 J. L. Liou, F. A. Lindholm, *Solid-State Electron., 30* (1987) 457–462.
11 S. R. Dhariwal and R. Grade, *Solid-State Electron., 27* (1984) 837–847.
12 F. A. Lindholm, J. J. Liou, A. Neugroschel and T. W. Jung, *IEEE Trans. Electron Devices, 34* (1987) 277–285.
13 S. C. Jain, E. L. Heasell and D. J. Roulston, *Prog. Quantum Electron., 11* (1987) 105–204.
14 V. K. Tewary and S. C. Jain, *Adv. Electron. Electron Phys., 67* (1986) 329–414.
15 A. Kapoor and L. S. Khothari, *J. Phys. D, 20* (1987) 1652–1656.
16 R. A. Moore, *RCA Rev., 40* (1980) 549–562.
17 S. C. Jain, S. K. Agarwal and Harsh, *J. Appl. Phys., 54* (1983) 3618–3619.
18 T. Jung, F. A. Lindholm and A. Neugroshel, *Sol. Cells, 22* (1987) 81–96.
19 S. C. Jain and R. Muralidharan, *Solid-State Electron., 24* (1981) 1147–1154.
20 J. P. Charles, I. Mekkaoui-Alaoui and G. Bordure, *Solid-State Electron., 28* (1985) 807–820.
21 S. M. Sze, *Physics of Semiconductor Devices*, 2nd edn, Wiley, New York, 1981.
22 A. Zondervan, L. A. Verhoef and F. A. Lindholm, *IEEE Trans. Electron Devices, 35* (1988) 85–88.
23 F. Pelanchon and P. Mialhe, *Solid-State Electron., 33* (1990) 47–51.
24 H. Reinhard, *Equations aux dérivées partielles*, Dunod Université, Paris, 1987.

Appendix

Equation (4) and boundary conditions given by eqns. (5), (6) and (7) constitute a typical Sturm–Liouville system [24]. The solution $\delta(x,t)$ can be expressed in the form:

$$\delta(x,t) = \sum_{p \geq 1} \frac{P_p(x)}{\sqrt{a_p}} T_p(t) \tag{A1}$$

with:

$$P_p(x) = \sin((\Omega_p/\sqrt{D_n})x) \tag{A2}$$

$$T_p(t) = T_p(0)\ \exp(-(1/\tau_n + \Omega_p{}^2)t) \tag{A3}$$

In eqns. (A2) and (A3), eigenvalue Ω_p is a solution of the following equation:

$$\tan((\Omega_p/\sqrt{D_n})H) = -(\sqrt{D_n}/S)\Omega_p \tag{A4}$$

and $\sqrt{a_p}$ is the norm of the eigenfunction P_p in the Hilbert space $L^2(0, H)$:

$$a_p = H/2 - \tfrac{1}{4}\sqrt{D_n}/\Omega_p\ \sin(2(\Omega_p/\sqrt{D_n})H) \tag{A5}$$

Note that eqn. (A4) implies restricted solutions in the form:

$$p\pi - \pi/2 < (\Omega_p/\sqrt{D_n})H \leq p\pi \tag{A6}$$

The pth coordinate, $T_p(0)$, of function $\delta(x,0)$ in the orthonormal base $(P_p(x)/\sqrt{a_p})p \geq 1$ of $L^2(0, H)$ reads:

$$T_p(0) = (\sqrt{a_p})^{-1} \int_0^H \delta(x,0)\ P_p(x)\ \mathrm{d}x \tag{A7}$$

The excess carrier concentration $\delta(x,0)$ satisfies eqn. (4) in the initial steady state:

$$D_n \partial^2 \delta(x,0)/\partial x^2 = \delta(x,0)/\tau_n \tag{A8}$$

This equation is easily solved with boundary conditions given by eqns. (6) and (7). The solution, $\delta(x,0)$, takes into account the illumination levels in both the initial and the final states, being a fundamental point of our method which has not been previously considered.

This mathematical analysis leads to the expression of function $\delta(x,t)$ in the form:

$$\delta(x,t) = \delta_\Phi \sum_{p \geq 1} \frac{\Omega_p}{a_p} \frac{\sqrt{D_n}}{1/\tau_n + \Omega_p{}^2} \sin((\Omega_p/\sqrt{D_n})x)\ \exp(-(1/\tau_n + \Omega_p{}^2)t) \tag{A9}$$

This expression of $\delta(x,t)$ is valid for solar cells with thin or thick bases, whatever the back surface recombination velocity may be (for an ohmic contact ($S = \infty$) the solution of eqn. (A4) is obvious).